Sources of dissolved organic matter during storm and inter-storm conditions in a lowland headwater catchment: constraints from high-frequency molecular data

L. Jeanneau[1], M. Denis[1], A-C. Pierson-Wickmann[1], G. Gruau[1], T. Lambert[1,*] and P. Petitjean[1]

[1]{UMR 6118 Géosciences Rennes, Université de Rennes 1/CNRS, 35042 Rennes, France}

[*]{now at: University of Liège, Institut de Physique (B5), B-4000 Sart Tilman}

Correspondence to: L. Jeanneau (Laurent.jeanenau@univ-rennes1.fr)

Abstract

The transfer of dissolved organic matter (DOM) at soil-river interfaces controls the biogeochemistry of micropollutants and the equilibrium between continental and oceanic C reservoirs. Then determining the transfer mechanisms of DOM is of main importance for ecological and geochemical reasons. Is stream DOM the result of the flushing of pre-existing soil DOM reservoirs activated by the modification of water flow paths? The evolution of the chemical composition of stream DOM investigated by thermally assisted hydrolysis and methylation (THM) using tetramethylammonium hydroxide (TMAH) coupled to a gas chromatograph and mass spectrometer (THM-GC-MS) during inter-storm conditions and five storm events with a high-frequency sampling gives new insights on this question. In inter-storm conditions, stream DOM is derived from the flushing of soil DOM, while during storm events, the modification of the distribution of chemical biomarkers allows the identification of three additional mechanisms. The first one corresponds to the destabilization of microbial biofilms by the increase in water velocity resulting in the fleeting export of a microbial pool. The second mechanism corresponds to the erosion of soils and river banks leading to a partition of organic matter between particles and dissolved phase. The third mechanism is linked to the increase in water velocity in soils that could induce the erosion of macropore walls, leading to an in-soil partitioning between soil microparticles and dissolved phase. The contribution of this in-soil erosive process would be linked to the magnitude of the hydraulic

gradient following the rise of water table and could persist after the recession, which could explain why the return to inter-storm composition of DOM does not follow the same temporal scheme as the discharge. Those results are of main importance to understand the transfer of nutrients and micropollutants at the soil-river interfaces during the hot moments that are storm events.

1 Introduction

The transfer of dissolved organic matter (DOM) at soil-river interfaces controls the biogeochemistry of micropollutants and the equilibrium between continental and oceanic C reservoirs (Corapcioglu and Jiang, 1993; Raymond et al., 2013). Then determining the transfer mechanisms of DOM is of main importance for ecological and geochemical reasons. The concentration of DOM generally decreasing from headwater to large river catchments (Ågren et al., 2007), there is nowadays a widely accepted consensus that a large proportion of river DOM ultimately come from headwater catchment soils (Billett et al., 2006; Morel et al., 2009). Unraveling the processes by which DOM is transferred from soils to headwater streams and understanding how these processes control the chemistry of the exported DOM are therefore two challenging issues of this research.

The export of soil DOM in headwater catchments is controlled by water flow paths which may change both at seasonal and event scales, depending on hydroclimatic conditions (Hinton et al., 1998). More than 60% of the dissolved organic carbon (DOC) exported annually is transferred during storm events highlighting them as hot moments in the continental C cycle (Morel et al., 2009). During storm events, the increase in discharge is associated with an increase in DOC concentrations (the parameter commonly used to quantify DOM concentrations) associated with changing flow path circulations due to the rise of water table, which results in the leaching of DOM-rich soil horizons (Maurice et al., 2002; McGlynn and McDonnell, 2003).

Storm events are also associated with changes in DOM composition and biodegradability (McLaughlin and Kaplan, 2013). Compositional changes have been recorded using different spectroscopic measurements namely UV-absorbance and fluorescence. The first results were obtained using low frequency spectroscopic measurements and have highlighted that DOM aromaticity increased during storm events (Hood et al., 2006; Maurice et al., 2002). It has been attributed to the mobilization of aromatic DOM from surface soil horizons with the rise of water table. However high frequency spectroscopic measurements have shown that concentration and composition were not linked and that the return to pre-event values was much longer for compositional indices than for concentration (Austnes et al., 2010; Knorr, 2013; Saraceno et al., 2009; Yang et al., 2013). This was interpreted as an evidence for in-stream production of fluorescing DOM (Austnes et al., 2010) or for a continuous contribution of surface soil horizons to the DOM export, even after the return to low-flow conditions (Strohmeier et al., 2013).

Molecular data investigating the differences in DOM composition between low-flow and high-flow conditions are less common than spectroscopic data, and comprise mostly low frequency lignin phenol data (Dalzell et al., 2005; Hernes et al., 2008). Those data on lignin phenols highlight a modification in the DOM composition with less-degraded lignins being mobilized during storm events. Since those modifications were correlated with the amount of suspended sediments in the water column, they have been interpreted as the mobilization of particles by erosion combined with partitioning of the lignin compounds between the solid and dissolved phase. This partitioning process could be linked to the in-stream production of fluorescing DOM suggested by Austnes et al. (2010). However those data have been acquired using low frequency water sampling strategies (one sample per storm event), and cannot be used therefore to investigate the persistence of the DOM aromatic fingerprint after storm events.

Thus, according to the existing database on DOM composition variation during storm events, it appears that the transfer of DOM in headwater catchments could not be regarded as simply the passive transfer of a surface soil DOM component leached by the water table rise. Other processes seems to be involved implying either a modification of the DOM composition on its way from its soil source to the stream or the involvement of additional DOM sources specifically generated and mobilized during the storm events. Answering these questions requires acquiring (i) high-frequency data on DOM composition during storm events, at a level sufficient to allow identification of theses possible additional sources and mechanisms and (ii) background information on the composition of soil organic matter (SOM), soil DOM and inter-storm river DOM. Moreover those data should be comparable with spectroscopic and molecular data available in the literature. Molecular data generated by thermally assisted hydrolysis and methylation (THM) using tetramethylammonium hydroxide (TMAH) coupled to a gas chromatograph and mass spectrometer (THM-GC-MS) seems to be particularly suitable. This technique can be used to simultaneously analyze phenol markers from lignins (LIG) and tannins (TAN), carbohydrates (CAR) and fatty acids (FA) (Grasset et al., 2009). LIG and TAN are commonly used to monitor the input of terrestrially-derived OM to oceans (Hedges and Parker, 1976) and their investigation has led to the partitioning process invoked for lignin compounds during storm events (Dalzell et al., 2005; Hernes et al., 2008). Analysis of CAR can differentiate between plant-derived and microbial inputs (Rumpel and Dignac, 2006) since the distribution of non-cellulosic monosaccharides is dominated by pentose (C5) for plant-derived inputs and by hexose (C6) and deoxyhexose (deoxyC6) for microbial inputs. Similar to CAR, the distribution of FA differs in plant-derived and microbial inputs (Cranwell, 1974; Eglinton and Hamilton, 1967; Lucas García et al., 2001; Matsuda and Koyama, 1977). The combination of those markers allows the investigation of the balance between microbial and plant-derived markers differentiating between soil DOM from organic-rich and organic-poor horizons in a wetland submitted to fluctuating water-table level and being correlated with the specific UV absorbance (SUVA) at 254 nm (Jeanneau et al., 2014).

In this study, high-frequency molecular data were obtained on five successive storm events that were sampled at the outlet of the Kervidy-Naizin catchment, a lowland headwater catchment occurring in Brittany, France. This catchment was preferentially selected due to previous studies on its hydrological responses to storm events (Aubert et al., 2013; Durand and Juan Torres, 1996; Morel et al., 2009), and on its DOM sources and transfer processes (Lambert et al., 2011, 2013, 2014; Morel et al., 2009). Moreover this study takes advantages of previous knowledge acquired during the hydrologic year 2010-2011 on (i) the temporal variations of the distribution of biomarkers, including lignin phenols, in soil DOM of the Mercy Wetland (France) that is the main contributor of DOM in the Kervidy catchment (Jeanneau et al., 2014; Morel et al., 2009) and (ii) the high-frequency sampling of stream water during winter storm events with previously investigated isotopic ($\delta^{13}C$) and hydrochemistry ([DOC], [Cl^-], [NO_3^-], [SO_4^{2-}]) data at the outlet of the Kervidy catchment (Lambert et al., 2014). Three main issues are addressed in this paper: (i) how does the molecular composition of DOM vary during one single storm event, and in between the five investigated storm events; do we see seasonal trends? ; (ii) is there a correlation between the variability of molecular biomarkers during storms and the variation of more global DOM characteristics such as the UV-absorbance? (iii) What new constraints do the molecular data set on the sources and transfer mechanisms of DOM during storms in this catchment?

2 Materials and methods

2.1 Site description

This research was conducted in the Kervidy-Naizin catchment which is a 4.9 km² lowland catchment located in central Brittany, western France (Figure 1). Numerous hydrological and biogeochemical studies have already been undertaken at this site, which belongs to a long-term monitoring research program aimed at understanding the impact of agricultural intensification and climate change on water pathways and water quality (Aubert et al., 2013; Lambert et al., 2013 and references therein). Only the information required for this study is presented here.

The Kervidy-Naizin catchment has a temperate oceanic climate. The mean annual temperature and precipitation (1993-2011) are 10.7°C and 814 mm, respectively. Rainfall events rarely exceed 20 mm per day, with 80% of rainfall events having an intensity of less than 4 mm per hour. The stream generally dries up from the end of August to October due to the small volume of water stored in the bedrock. The high-flow stage generally lasts from December to April, with maximum discharges occurring during February and March.

The elevation ranges from 93 to 135 m above sea level, with hillslope gradients of less than 5%. The soils are silty loams, with depths ranging from 0.5 to 1.5 m, and are classified as Stagnic fluvisols (IUSS Working Group WRB, 2006) developed from alluvial material and Brioverian schists. The aquifer in the Kervidy-Naizin catchment consists mainly of the unconsolidated weathered bedrock, the deeper fresh bedrock, though locally fractured, being generally considered impermeable. In this aquifer, the groundwater flows from upland down to bottom land all the year round and feeds the stream. Along hillslopes, the water table depth is typically 0-10 m. In bottom land areas, the water table is near the soil surface during the wet season and the uppermost layer of the groundwater thus flows through the organic-rich horizon of the soils. The surface area of this domain of interaction between the organic-rich part of soils and the groundwater flow depends strongly on the hydroclimatic conditions. During dry hydrologic years, it may be restricted to the riparian, wetland domains representing less than 5% of the total catchment area. During wet hydrological years, the upper limit moves upwards in the hillslopes, and the surface area of this domain may increase up to 20% of the total catchment surface area (Crave and Gascuel-Odoux, 1997).

Previous studies have evidenced the occurrence of three distinct hydrological periods in the Kervidy-Naizin on the basis of the seasonality of water table depth fluctuations in wetland and upland domains (Lambert et al., 2013; Molenat et al., 2008). First, after the dry summer, the water table starts to rise in the riparian zone but remains deep in the upland domain (period A). Second, as precipitation increases, the water table rises in the upland domain resulting in the establishment of a hydrological connection between riparian and upland domains and the subsequent increase of upland groundwater flow towards the riparian zone (period B). Third, in late spring and during summer, upland groundwater flow decreases progressively resulting in a gradual air-drying of wetland soils (period C).

2.2 Previous data

2.2.1 Molecular data on SOM and soil DOM

The molecular composition of SOM and the spatio-temporal variation of the molecular composition of soil DOM were investigated in the central, most widespread wetland zone of the catchment (so-called Mercy wetland) during the hydrologic year 2010-2011 (Jeanneau et al., 2014). Concerning SOM, the proportion of LIG-TAN, CAR and FA were 16, 29 and 55 % and 4, 3 and 93 % in the organo-mineral and mineral horizons, respectively. The deoxyC6/C5 ratio was 0.4 and 0.2 in the organo-mineral and mineral horizons, respectively and the proportion of plant-derived markers was 88 and 71 % in the organo-mineral and mineral horizons, respectively.

During hydrologic period B, when the five studied storm events were sampled, there was a clear differentiation between surface (10 cm) and deep (50 cm) soil DOM. In the surface horizons, the proportion of plant-derived markers remained higher than 70% with a mean value of 0.8±0.1 (standard deviation) for the ratio deoxyC6/C5 while in the deep horizon, this proportion was lower than 30% with a mean value of 1.3±0.2 (standard deviation) for the ratio deoxyC6/C5. Molecular data were well correlated along the depth profile with SUVA values at 254 nm (SUVA against deoxyC6/C5, $R^2 = 0.75$, p-value < 0.0001, n = 37) that exhibited a clear differentiation between soil DOM sampled in surface (4.1 ± 0.4 L mg^{-1} m^{-1}) and deep (2.5 ± 0.7 L mg^{-1} m^{-1}) horizons (Lambert et al., 2013).

2.2.2 Previous data on river samples

The composition of DOM in the river during the five studied storm events was previously investigated using $\delta^{13}C$ values (Lambert et al., 2014). The intra-storm variability of $\delta^{13}C$ values ranged between the values recorded in the soil solution of the organic-rich surface horizon at the beginning of storm events and of the organic-poor deep horizon at the end of storm events. Those data were in accordance with the end member mixing approach (EMMA) developed using nitrate, sulfate and DOC concentrations in order to determine the contributions of rain water, deep groundwater, shallow riparian groundwater and hillslope groundwater. The storm-flow generation was decomposed in three successive steps: (i) an overland flow above the saturated wetland soil horizons; (ii) a subsurface flow through the uppermost organic-rich horizon of wetland soils; and (iii) a subsurface return flow from shallow hillslope groundwater flowing through deeper organic-poor horizon of wetland soils (Lambert et al., 2011, 2014). Those data tend to support the concept of a storm-DOM flux generated by the mobilization of pre-existing DOM pools via the rise of the water table.

2.3 Sampling

Soils from the Mercy wetland were sampled using a hand auger on October 2010. Three sample subsets were collected in the organo-mineral (0-10 cm) and the mineral (30-40 cm) horizons. After removal of roots and gravels by eye, all samples were freeze-dried and crushed using an agate mortar.

The five studied storm events were sampled between December 04, 2010 and February 19, 2011, during hydrological period B (Figure 2). Their numbering corresponds to those used in the previous paper by Lambert et al. (2014). Events 2, 3, 4, 5 and 6 were sampled on December 4, December 19, January 6, February 13 and February 19, respectively. Stream discharge was recorded every minute with an automatic gauge station located at the outlet of the catchment. The beginning and the end of a flood are determined respectively by an increase and a decrease of the stream discharge of > 1 L s^{-1} in 10 min at the stage recorder. Turbidity was monitored using an APC-TU Ponselle sensor with a measure every 30 seconds averaged every 10 minutes. Rainfall amounts are continuously monitored on an hourly interval basis using a weather station located ca. 300 m away from the catchment outlet. Storm stream water samples (1 L) were collected 0.4 m above the river bed using a refrigerated (4°C) automatic sampler (Sigma 900 Max) installed in a technical hut located at the outlet of the catchment (Figure 1) and were stored in polypropylene (PP) bottles. Sampling frequency during the monitored storm events varied from one sample every 30 min to one sample every hour, depending on the hydrograph variations. Base-flow waters between each storm event were collected manually on a daily basis (5 p.m.) in 60 mL PP bottles for DOC monitoring and fortnightly in 1 L glass bottles for isotopic and molecular investigations. Stream water was filtered at 0.22 µm using cellulose acetate membrane filters previously washed with 500 mL of de-ionized water and few mL of the sample itself. Filtered water samples were then acidified using 1 N HCl (1 mL per L of sample) to remove inorganic carbon, and finally frozen and freeze-dried.

2.4 Analytical procedure

Approximately 2 mg of solid residue (soil or lyophilizate) was introduced into an 80 µL aluminum reactor with an excess of solid tetramethylammonium hydroxide (TMAH – ca. 10 mg). The THM reaction was performed on-line using a vertical micro-furnace pyrolyser PZ-2020D (Frontier Laboratories, Japan) operating at 400°C during 1 min. The products of this reaction were injected into a gas chromatograph (GC) GC-2010 (Shimadzu, Japan) equipped with a SLB 5MS capillary column (60 m × 0.25 mm ID, 0.25 µm film thickness) in the split mode. The split ratio was adapted according to the sample and ranged from 15 to 30. The temperature of the transfer line was 321°C and the temperature of the injection port was 310°C. The oven temperature was programmed from an initial temperature of 50°C (held for 2 min) rising to 150°C at 15°C/min, then rising from 150°C to 310°C (held for 14 min) at 3°C/min. Helium was used as the carrier gas, with a flow rate of 1.0 ml/min. Compounds were detected using a QP2010+ mass spectrometer (MS) (Shimadzu, Japan) operating in the full scan mode. The temperature of the transfer line was set at 280°C, and molecules were ionized by electron impact using an energy of 70 eV. The temperature of the ionization source was set at 200°C. The list of analyzed compounds and m/z ratios used for their integration are given in the supplementary materials (Table S1). Compounds were identified on the basis of their full-scan mass spectra by comparison with the NIST library and with published data. They were classified into three categories: lignin (LIG) and tannin (TAN) markers, carbohydrates (CAR) and fatty acids (FA). The peak area of the selected m/z for each compound was integrated and corrected by a mass spectra factor (MSF) calculated as the reciprocal of the proportion of the fragment (used for the integration) relating to the entire fragmentogram provided by the NIST library. The proportion of each compound class was calculated by dividing the sum of the areas of the compounds in this class by the sum of the peak areas of all analyzed compounds multiplied by 100 in order to express it as a percentage. Since no internal standard were used, these data must be handled in a qualitative way. Five samples were analyzed in triplicate in order to investigate the experimental repeatability of the analysis. The relative standard deviation (RSD) calculated for CAR proxy, LIG proxies and the proportion of plant-derived markers was 9, 10 and 6%, respectively. The uncertainties given in Figures 3, 4, 5 and S1 correspond to these mean RSD values. The use of THM-GC-MS to investigate the temporal variability of the DOM composition meant that it was necessary to assume that the ionization efficiency and matrix effects are equivalent for all analyzed compounds in all samples.

2.5 Treatment of molecular data

The classification of molecular markers generated by THM-GC-MS into microbial and plant-derived markers has been performed according to Jeanneau et al. (2014). Briefly, the analyzed compounds were classified as follow. LIG-TAN are characteristic of DOM inherited from plant-derived inputs whereas CAR and FA can be inherited from both plant-derived and microbial sources. The proportion of microbial CAR was calculated using an end-member mixing approach (EMMA) based on the deoxyC6/C5 ratio, assuming that it is 0.5 and 2.0 for plant-derived and microbial inputs, respectively (Rumpel and Dignac, 2006). C6 were not considered since they can derive from the THM of cellulose leading to an increase of the plant-derived C6 signal. The proportion of microbial FA was calculated as the % low molecular weight FA (< C19) by excluding C16:0 and C18:0 that can be inherited from plant-derived or microbial inputs. The microbial FA were composed of C12:0, C13:0, C14:0, C15:0, C17:0, *anteiso* and *iso* C15:0 and C17:0, *iso* C16:0, C16:1 and C18:1 commonly used as bacterial indicators (Frostegård et al., 1993). The proportion of microbial markers was calculating as the sum of the proportion of microbial CAR multiplied by the proportion of CAR plus the proportion of microbial FA multiplied by the proportion of FA. From this value, it is possible to calculate the proportion of plant-derived markers among the analyzed compounds. For this calculation, it is assumed that the modification of the distribution of CAR and FA would only be due to the relative proportion between these plant-derived and microbial inputs. Although these assumptions still need to be validated by investigating pure and known mixtures of vegetal and microbial sources, this approach can be used to approximate the proportions of plant-derived and microbial CAR.

3 Results

3.1 Soils and soil solution

Compared with its companion study (Jeanneau et al., 2014), compositional ratio on LIG-TAN markers were calculated for SOM and soil DOM. In SOM, the ratio C/V, that is the ratio of the sum of coumaric acid and ferulic acid on the sum of vanillic acid, vanilline and acetovanillone, was 1.3 and 1.6 in surface and deep horizons, respectively. The ratio Ac/Al (V), that is the ratio of vanillic acid on vanilline, was 2.6 and 1.6 in surface and deep horizons, respectively. In soil DOM from November 29, 2010 to March 11, 2011, the C/V ratio ranged from 0.2 to 0.4 in the surface horizon and remained stable at 0.2 in the deep horizon. The Ac/Al (V) ratio ranged from 7.1 to 12.1 (9.1 ± 1.7, mean value ± standard deviation) in the surface horizon and from 3.6 to 6.9 (4.7 ± 1.2, mean value ± standard deviation) in the deep horizon.

3.2 River DOM in inter-storm conditions

In river samples from November 28, 2010 to March 8, 2011, the proportion of plant-derived markers ranged from 34 to 48% of the analyzed compounds (Figure 3). Among CAR, the ratio deoxyC6/C5 ranged from 1.0 to 1.6 and heptoses have never been detected in those samples. For LIG-TAN, the C/V ratio remained lower than 0.2 with the exception of the sampling of January 7, 2011 with a value of 0.5. The Ac/Al (V) ratio ranged from 4.5 to 7.7.

3.3 River DOM during storm events

During the five recorded storm events, the composition of DOM was modified as highlighted by isotopic (Lambert et al., 2014), spectroscopic and molecular markers analyses (Figures 4 and S1, Table 1). The modifications were similar for the five storm events. At the beginning of storm events, the first sample was characterized by low values of SUVA at 254 nm comprised between 2.0 and 2.8, depending of the storm event. Then this value increased from the second sample and remained stable up to the end of the sampling. The higher SUVA values were 3.0 (event 6), 3.2 (event 2), 3.3 (event 5), 3.4 (event 3) and 3.5 (event 4).

At the molecular level, during the five recorded storm events, the proportion of plant-derived makers among the analyzed compounds has increased (Figure 5). The initial value was 31 (events 2, 4 and 6), 49 (event 3) and 14 % (event 5). It increased with the discharge and reached its maximum with the peak flow. This maximum value ranged from 63 (event 6) to 82 % (event 3). After the peak flow, the proportion of plant-derived markers decreased regularly of approximately 10 % (events 2, 4, 5 and 6) or remained stable (event 3) up to the end of the recording.

The composition of CAR, recorded by the deoxyC6/C5 ratio, was also modified during storm events. The initial value was 1.5 (event 3), 1.6 (event 2 and 4), 1.9 (event 6) and 2.7 (event 5). This ratio decreased with the increase of discharge, reached its minimal value at the peak flow and remained stable up to the end of the recording. Among CAR, heptoses were detected in the first sample at the beginning of the storm events and up to the fifth sample for the event 2 (Figure S2).

The composition of LIG-TAN, recorded by the C/V and Ac/Al (V) ratios, was modified during storm events. The C/V ratio increased with the discharge from 0.2 at the beginning of storm events to 0.5 (event 5), 0.6 (events 2 and 4), 0.7 (event 3) and 0.8 (event 6). Depending of the storm event, this value slightly decreased or remained stable up to the end of the recording. The evolution of the Ac/Al (V) ratio was storm-dependant. For the events 2, 4 and 6, it remained stable around 5.0 with extreme values that could be considered as outliers, while for the events 3 and 5, it decreased from 7.0 to 5.0 with the increase of the discharge and then remained stable up to the end of the recording.

4 Discussion

4.1 Inter-storm stream DOM

The molecular composition of inter-storm stream DOM samples was characterized by values comprised between soil DOM from the organic-rich and the organic-poor horizons. This is in agreement with the flowpath geometry during inter-storm conditions, with the wetland being saturated and the lower mineral soil horizon characterized by an hydraulic pressure higher than the upper organic-mineral horizon. Since the proportion of plant-derived markers clearly differentiated soil DOM from organo-mineral and mineral horizons and was fairly stable during the investigated period (Jeanneau et al., 2014), it can be used in an end member mixing approach in order to determine the proportions of DOM coming from organo-mineral and mineral horizons. From November 29, 2010 to March 11, 2011 the proportion of stream

DOM originating from organo-mineral horizon ranged from 23 and 59 % (37 ± 13%, average ± standard error), which is in line with the conclusions of Strohmeier et al. (2013) stating that upper organic-rich soils in riparian wetland zones are important DOM contributors, even in non-storm conditions.

4.2 Beginning of floods: export of a microbial pool

At the beginning of the storm events the proportion of plant-derived markers in stream DOM was lower than in stream DOM during antecedent inter-storm conditions. The highest value recorded for event 3 was probably due to the 62% increase (from 48 to 78 l s^{-1}) of the discharge recorded the day before the event (Table S2). The stream DOM at beginning of storm events was also characterized by higher deoxyC6/C5 ratio than inter-storm stream DOM and by the occurrence of heptoses. Heptoses have been quantified in microbial exopolysaccharides (Jiao et al., 2010) and lipopolysaccharides (Sadovskaya et al., 1998). This export of a microbial pool as denoted by the high concentrations in heptoses and other microbial-derived biomarkers was the most important for event 5 with 86% of the analyzed biomarkers being from microbial origin during the earliest stages of this event. This was the first flood after the establishment of reducing conditions in wetland soils (Lambert et al., 2013), when the riparian wetland zones located at the soil-river interface played the role of a hotspot for iron biogeochemical reduction processes.

This microbial pool could derived from the microbial lysis occurring in soils over the dry period and that would have been flushed during the wetting-up phase (Christ and David, 1996). However the five recorded storm events were during the hydrological phase B characterized by permanent waterlogging of riparian wetland soils. As a consequence the wetting-up phase, denoted A, had already occurred. Moreover heptoses were not detected nor in soil DOM nor in stream DOM sampled in inter-storm conditions. Then those compounds could be characteristic of microbial biofilms that likely developed in these zones at that time either directly in the soil macroporosity or at the wetland-stream interface (Knorr, 2013), and that could have been destabilized and transported into the stream by the increase of water velocity (Trulear and Characklis, 1982) at the beginning of storm events.

The export of this microbial pool at the beginning of storm events could perhaps be responsible for the extreme value recorded using high-frequency fluorescence measurements. The first storm samplings are often associated with high contributions of protein-like chromophore and low contribution of humic-like chromophores (Knorr, 2013), high fluorescence index and low SUVA (Inamdar et al., 2011; Vidon et al., 2008).

4.3 Soil erosion as a DOM producer

During the five monitored storm events, the compositional ratios calculated on LIG were modified. The C/V ratio increased from 0.2 to 0.8 and the Ac/Al (V) ratio decreased from 7 to 5 with the exception of event 6 where it remained stable around 5. Those modifications of the composition of LIG transferred from soils to rivers during flood events are in accordance with data on lignin phenols obtained along the Big Pine Creek watershed (Dalzell et al., 2005) and the Willow Slough watershed (Hernes et al., 2008). In both of those watersheds, storm stream DOM was characterized by higher C/V and lower Ac/Al (V) ratios than DOM sampled in inter-storm conditions. Although the differences in analytical techniques makes the comparison of data difficult (Wysocki et al., 2008), the compositional ratios evolve similarly during the biodegradation process with a decrease for the C/V ratio and an increase for the Ac/Al (V) ratio (Kabuyah et al., 2012; Vane et al., 2005). The aforementioned modifications of C/V and Ac/Al (V) ratios have then been attributed to the mobilization of less-degraded lignins during flood events (Dalzell et al., 2005; Hernes et al., 2008).

The values of the C/V ratio recorded during storm events were higher than the values in soil solutions. Thus stream DOM recorded during storm events cannot be viewed simply as resulting from the passive transfer of soil DOM to the stream. Among the different constituents analyzed so far in the catchment, only the SOM presented C/V values that could explain the high storm DOM values (Figure 6). In the Willow Slough catchment, the concentration in lignin markers has been shown to be correlated to the concentration in suspended matter indicating that DOM transferred during storm events can be, in part, inherited from the partitioning of organic compounds between solid and dissolved phases (Hernes et al., 2008). Such a correlation between lignin compounds and suspended sediment was also found in the present study, as highlighted by the regression between turbidity and the C/V ratio (Figure 7). Thus, soil erosion and the equilibrium between solid (soil particles) and liquid (river) phases is likely to be an additional source of DOM transferred from soil to rivers during storm events. However, this positive relationship was only found for the samples collected during the rising limb of the hydrograph (grey square, $R^2 = 0.68$, p-value < 0.0001, $n = 23$). After the peak discharge, turbidity decreased while the C/V ratio remained high leading to a poor correlation when all the samples are considered (black square, $R^2 = 0.11$, p-value =

0.008, n = 64). This highlights that the aforementioned soil erosion process alone cannot explain the persistence of high C/V ratios during the falling limb of the hydrograph. Since the complementary DOM production process must have let the C/V ratio high and that the only component that brings a high C/V is SOM, it should be similar to soil erosion, that is to say consisting of a transfer of SOM-born components into the circulating water. This could come from the destabilization and the disaggregation of soil aggregates during the erosion of macropores walls due to the increase in water velocity during storm event (Wilson et al., 2005) that could lead to a modification of the composition of DOM produced within the different soil horizons.

4.4 Temporal scheme of DOM producing processes during storm events

The increase in the proportion of aromatic DOM during the rising limb of the hydrograph that remained high even after the recession as observed in the present study has been described under different climates and for different catchments (Austnes et al., 2010; Knorr, 2013; Singh et al., 2015). It is then probable that the succession of DOM producing mechanisms leading to this pattern can be generalized. The combination of previous and present results could be used to decompose this succession into four distinct mechanisms. In inter-storm conditions, DOM would be derived from the passive (without compositional changes of the DOM during transport) flushing of organic-rich and organic-poor wetland soil horizons. The contribution of each soil horizon would be controlled by the water table level. During a rain event, the increase in water velocity would induce the destabilization of microbial biofilms resulting in the export of a microbial pool. This first stage would be followed by the rise of the water table, which in association with the decrease of lateral hydraulic conductivity with depth (Seibert et al., 2009) would induce an increase of the proportion of the water flowing through the upper organic-rich wetland surface horizon. This would result in an increase of the stream DOC concentration. In the same time, erosion of soils and river banks would induce an increase of the turbidity leading to a partition of organic matter between particles and dissolved phase. The contribution of this soil surface erosive process on the DOM chemistry would depend on the concentration in suspended matter and would therefore decrease during the falling limb of the hydrograph. In the same time, the increase in water velocity in soils could induce the erosion of macropore walls, leading to an in-soil partitioning between soil microparticles and dissolved phase. The contribution of this in-soil erosive process would be linked to the magnitude of the hydraulic gradient following the rise of water table. Since the recovery of pre-event conditions is longer for in-soil hydraulic gradient than for discharge (Lambert et al., 2014 – Fig 3.b), this could explain why the compositional proxies, including biomarkers and spectroscopic measurements, do not recover their pre-event values with the same kinetic as stream DOC concentrations. Sampling soil solutions during storm events and up to the recovery of pre-event values at the same high frequency than deployed for monitoring stream variations would be necessary to test this in-soil erosive process.

4.5 Summary and implications

The results from this study thus highlight changes in DOM sources and DOM transfer processes during storm and inter-storm conditions. Although the source of DOM during inter-flow conditions appears to have been the DOM contained in the soil horizons of the riparian wetland zones which was passively transferred into the stream, the DOM source and DOM transfer processes were more complex during storm periods. During these periods, the DOM transferred from soil to the stream was not only due to the flush of DOM already occurring in soils but also to additional sources and production processes that lead to the occurrence of less-degraded molecules in the dissolved phase. Those findings, which appear characteristic of DOM transfer in lowland catchments worldwide as far as the current literature is concerned, have two important implications.

The first one concerns the transfer of micropollutants, which is mainly controlled by the complexing properties of OM. The partitioning between soil particles and the dissolved phase during storm event highlighted in this study induced the occurrence in the dissolved phase of less-biodegraded molecules, that is to say a DOM of more hydrophobic composition (Kleber and Johnson, 2010). SOM hydrophobicity is assumed to be the main driving force of the retention of hydrophobic micropollutants in soils, such as many pesticides and antibiotics (Ji et al., 2011). This DOM producing process could therefore lead to hot moments in the transfer of these harmful compounds from soils to the dissolved phase of stream water increasing their bioavailability and then their potential for creating undesirable effects, such as antibiotic resistance (Hellweger et al., 2011).

The second implication concerns the modeling of the export of DOM from headwater catchment. In lowland headwater catchments, up to 80% of DOM is transferred during storm events (Raymond and Saiers, 2010). In many modeling studies, it is assumed that the DOM transfer process during storm events consists of the flushing of pre-existing soil pools. Since the latter are calibrated in term of size (concentration) and nature (composition) using samples taken in inter-storm conditions, these models don't take into account additional DOM producing processes which could occur during the water transfer process, such as the surface and subsurface erosion processes suggested here. This lack could explain why modeling studies succeed in reproducing inter-storm DOM concentrations, but not storm flow DOM contents (Birkel et al., 2014). Increased interactions between geochemists and modelers should help in improving DOM export modeling.

Acknowledgements

We thank the technical staff from INRA and Géosciences Rennes for their assistance during the fieldwork. This research was funded by the University of Rennes 1 through the "Varia-MOD" project and by the CNRS through the EC2CO "Prodynamos" project. We used data provided online by the environmental observatory ORE AgrHys (www6.inra.fr/ore_agrhys_eng/).

References

Ågren, A., Buffam, I., Jansson, M. and Laudon, H.: Importance of seasonality and small streams for the landscape regulation of dissolved organic carbon export, J. Geophys. Res. Biogeosciences, 112(G3), G03003, 2007.

Aubert, A. H., Gascuel-Odoux, C., Gruau, G., Akkal, N., Faucheux, M., Fauvel, Y., Grimaldi, C., Hamon, Y., Jaffrézic, A., Lecoz-Boutnik, M., Molénat, J., Petitjean, P., Ruiz, L. and Merot, P.: Solute transport dynamics in small, shallow groundwater-dominated agricultural catchments: insights from a high-frequency, multisolute 10 yr-long monitoring study, Hydrol Earth Syst Sci, 17(4), 1379–1391, 2013.

Austnes, K., Evans, C., Eliot-Laize, C., Naden, P. and Old, G.: Effects of storm events on mobilisation and in-stream processing of dissolved organic matter (DOM) in a Welsh peatland catchment, Biogeochemistry, 99(1-3), 157–173, 2010.

Billett, M. F., Deacon, C. M., Palmer, S. M., Dawson, J. J. C. and Hope, D.: Connecting organic carbon in stream water and soils in a peatland catchment, J. Geophys. Res. Biogeosciences, 111(G2), G02010, 2006.

Birkel, C., Soulsby, C. and Tetzlaff, D.: Integrating parsimonious models of hydrological connectivity and soil biogeochemistry to simulate stream DOC dynamics, J. Geophys. Res. Biogeosciences, 119(5), 2013JG002551, 2014.

Christ, M. J. and David, M. B.: Temperature and moisture effects on the production of dissolved organic carbon in a Spodosol, Soil Biol. Biochem., 28(9), 1191–1199, 1996.

Corapcioglu, M. Y. and Jiang, S.: Colloid-facilitated groundwater contaminant transport, Water Resour. Res., 29(7), 2215–2226, 1993.

Cranwell, P. A.: Monocarboxylic acids in lake sediments: Indicators, derived from terrestrial and aquatic biota, of paleoenvironmental trophic levels, Chem. Geol., 14(1–2), 1–14, 1974.

Crave, A. and Gascuel-Odoux, C.: The influence of topography on time and space distribution of soil surface water content, Hydrol. Process., 11(2), 203–210, 1997.

Dalzell, B. J., Filley, T. R. and Harbor, J. M.: Flood pulse influences on terrestrial organic matter export from an agricultural watershed, J Geophys Res, 110(G2), G02011, 2005.

Durand, P. and Juan Torres, J. L.: Solute transfer in agricultural catchments: the interest and limits of mixing models, J. Hydrol., 181(1–4), 1–22, 1996.

Eglinton, G. and Hamilton, R. J.: Leaf epicuticular waxes, Science, 156(3780), 1322–1335, 1967.

Frostegård, Å., Tunlid, A. and Bååth, E.: Phospholipid Fatty Acid Composition, Biomass, and Activity of Microbial Communities from Two Soil Types Experimentally Exposed to Different Heavy Metals, Appl. Environ. Microbiol., 59(11), 3605–3617, 1993.

Grasset, L., Rovira, P. and Amblès, A.: TMAH-preparative thermochemolysis for the characterization of organic matter in densimetric fractions of a Mediterranean forest soil, J. Anal. Appl. Pyrolysis, 85(1-2), 435–441, 2009.

Hedges, J. I. and Parker, P. L.: Land-derived organic matter in surface sediments from the Gulf of Mexico, Geochim. Cosmochim. Acta, 40(9), 1019–1029, d1976.

Hellweger, F. L., Ruan, X. and Sanchez, S.: A Simple Model of Tetracycline Antibiotic Resistance in the Aquatic Environment (with Application to the Poudre River), Int. J. Environ. Res. Public. Health, 8(2), 480–497, 2011.

Hernes, P. J., Spencer, R. G. M., Dyda, R. Y., Pellerin, B. A., Bachand, P. A. M. and Bergamaschi, B. A.: The role of hydrologic regimes on dissolved organic carbon composition in an agricultural watershed, Geochim. Cosmochim. Acta, 72(21), 5266–5277, 2008.

Hinton, M. J., Schiff, S. L. and English, M. C.: Sources and flowpaths of dissolved organic carbon during storms in two forested watersheds of the Precambrian Shield, Biogeochemistry, 41(2), 175–197, 1998.

Hood, E., Gooseff, M. N. and Johnson, S. L.: Changes in the character of stream water dissolved organic carbon during flushing in three small watersheds, Oregon, J Geophys Res, 111(G1), G01007, 2006.

Inamdar, S., Singh, S., Dutta, S., Levia, D., Mitchell, M., Scott, D., Bais, H. and McHale, P.: Fluorescence characteristics and sources of dissolved organic matter for stream water during storm events in a forested mid-Atlantic watershed, J Geophys Res, 116(G3), G03043, 2011.

IUSS Working Group WRB: World reference base for soil resources 2006, World Soil Resources Reports No. 103. FAO, Rome, 2006.

Jeanneau, L., Jaffrezic, A., Pierson-Wickmann, A.-C., Gruau, G., Lambert, T. and Petitjean, P.: Constraints on the Sources and Production Mechanisms of Dissolved Organic Matter in Soils from Molecular Biomarkers, Vadose Zone J., 13(7), 2014.

Jiao, Y., Cody, G. D., Harding, A. K., Wilmes, P., Schrenk, M., Wheeler, K. E., Banfield, J. F. and Thelen, M. P.: Characterization of Extracellular Polymeric Substances from Acidophilic Microbial Biofilms, Appl. Environ. Microbiol., 76(9), 2916–2922, 2010.

Ji, L., Wan, Y., Zheng, S. and Zhu, D.: Adsorption of Tetracycline and Sulfamethoxazole on Crop Residue-Derived Ashes: Implication for the Relative Importance of Black Carbon to Soil Sorption, Environ. Sci. Technol., 45(13), 5580–5586, 2011.

Kabuyah, R. N. T. M., van Dongen, B. E., Bewsher, A. D. and Robinson, C. H.: Decomposition of lignin in wheat straw in a sand-dune grassland, Soil Biol. Biochem., 45(0), 128–131, 2012.

Kleber, M. and Johnson, M. G.: Advances in Understanding the Molecular Structure of Soil Organic Matter: Implications for Interactions in the Environment, Advances in Agronomy, 106, 77–142, 2010.

Knorr, K.-H.: DOC-dynamics in a small headwater catchment as driven by redox fluctuations and hydrological flow paths – are DOC exports mediated by iron reduction/oxidation cycles?, Biogeosciences, 10(2), 891–904, 2013.

Lambert, T., Pierson-Wickmann, A.-C., Gruau, G., Thibault, J.-N. and Jaffrezic, A.: Carbon isotopes as tracers of dissolved organic carbon sources and water pathways in headwater catchments, J. Hydrol., 402(3–4), 228–238, 2011.

Lambert, T., Pierson-Wickmann, A.-C., Gruau, G., Jaffrezic, A., Petitjean, P., Thibault, J.-N. and Jeanneau, L.: Hydrologically driven seasonal changes in the sources and production mechanisms of dissolved organic carbon in a small lowland catchment, Water Resour. Res., 49, 1–12, 2013.

Lambert, T., Pierson-Wickmann, A.-C., Gruau, G., Jaffrezic, A., Petitjean, P., Thibault, J. N. and Jeanneau, L.: DOC sources and DOC transport pathways in a small headwater catchment as revealed by carbon isotope fluctuation during storm events, Biogeosciences, 11(11), 3043–3056, 2014.

Lucas García, J. A., Barbas, C., Probanza, A., Barrientos, M. L. and Gutierrez Mañero, F. J.: Low molecular weight organic acids and fatty acids in root exudates of two Lupinus cultivars at flowering and fruiting stages, Phytochem. Anal., 12(5), 305–311, 2001.

Matsuda, H. and Koyama, T.: Early diagenesis of fatty acids in lacustrine sediments—II. A statistical approach to changes in fatty acid composition from recent sediments and some source materials, Geochim. Cosmochim. Acta, 41(12), 1825–1834, 1977.

Maurice, P. A., Cabaniss, S. E., Drummond, J. and Ito, E.: Hydrogeochemical controls on the variations in chemical characteristics of natural organic matter at a small freshwater wetland, Chem. Geol., 187(1–2), 59–77, 2002.

McGlynn, B. L. and McDonnell, J. J.: Role of discrete landscape units in controlling catchment dissolved organic carbon dynamics, Water Resour Res, 39(4), 1090, 2003.

McLaughlin, C. and Kaplan, L. A.: Biological lability of dissolved organic carbon in stream water and contributing terrestrial sources, Freshw. Sci., 32(4), 1219–1230, 2013.

Molenat, J., Gascuel-Odoux, C., Ruiz, L. and Gruau, G.: Role of water table dynamics on stream nitrate export and concentration in agricultural headwater catchment (France), J. Hydrol., 348(3–4), 363–378, 2008.

Morel, B., Durand, P., Jaffrezic, A., Gruau, G. and Molenat, J.: Sources of dissolved organic carbon during stormflow in a headwater agricultural catchment, Hydrol. Process., 23(20), 2888–2901, 2009.

Raymond, P. and Saiers, J.: Event controlled DOC export from forested watersheds, Biogeochemistry, 100(1-3), 197–209, 2010.

Raymond, P. A., Hartmann, J., Lauerwald, R., Sobek, S., McDonald, C., Hoover, M., Butman, D., Striegl, R., Mayorga, E., Humborg, C., Kortelainen, P., Durr, H., Meybeck, M., Ciais, P. and Guth, P.: Global carbon dioxide emissions from inland waters, Nature, 503(7476), 355–359, 2013.

Rumpel, C. and Dignac, M.-F.: Gas chromatographic analysis of monosaccharides in a forest soil profile: Analysis by gas chromatography after trifluoroacetic acid hydrolysis and reduction–acetylation, Soil Biol. Biochem., 38(6), 1478–1481, 2006.

Sadovskaya, I., Brisson, J.-R., Lam, J. S., Richards, J. C. and Altman, E.: Structural elucidation of the lipopolysaccharide core regions of the wild-type strain PAO1 and O-chain-deficient mutant strains AK1401 and AK1012 from Pseudomonas aeruginosa serotype O5, Eur. J. Biochem., 255(3), 673–684, 1998.

Saraceno, J. F., Pellerin, B. A., Downing, B. D., Boss, E., Bachand, P. A. M. and Bergamaschi, B. A.: High-frequency in situ optical measurements during a storm event: Assessing relationships between dissolved organic matter, sediment concentrations, and hydrologic processes, J Geophys Res, 114, G00F09, 2009.

Seibert, J., Grabs, T., Köhler, S., Laudon, H., Winterdahl, M. and Bishop, K.: Linking soil- and stream-water chemistry based on a Riparian Flow-Concentration Integration Model, Hydrol Earth Syst Sci, 13(12), 2287–2297, 2009.

Singh, S., Inamdar, S. and Mitchell, M.: Changes in dissolved organic matter (DOM) amount and composition along nested headwater stream locations during baseflow and stormflow, Hydrol. Process., 29(6), 1505-1520, 2015.

Strohmeier, S., Knorr, K.-H., Reichert, M., Frei, S., Fleckenstein, J. H., Peiffer, S. and Matzner, E.: Concentrations and fluxes of dissolved organic carbon in runoff from a forested catchment: insights from high frequency measurements, Biogeosciences, 10(2), 905–916, 2013.

Trulear, M. G. and Characklis, W. G.: Dynamics of biofilm processes, J. Water Pollut. Control Fed., 54(9), 1288–1301, 1982.

Vane, C. H., Drage, T. C., Snape, C. E., Stephenson, M. H. and Foster, C.: Decay of cultivated apricot wood (Prunus armeniaca) by the ascomycete Hypocrea sulphurea, using solid state 13C NMR and off-line TMAH thermochemolysis with GC–MS, Int. Biodeterior. Biodegrad., 55(3), 175–185, 2005.

Vidon, P., Wagner, L. and Soyeux, E.: Changes in the character of DOC in streams during storms in two Midwestern watersheds with contrasting land uses, Biogeochemistry, 88(3), 257–270–270, 2008.

Wilson, G. V., Xu, M., Chen, Y., Liu, G. and Römkens, M. J. M.: Macropore flow and mass wasting of gullies in the Loess Plateau, China, Int. J. Sediment Res., 20(3), 249–258, 2005.

Wysocki, L. A., Filley, T. R. and Bianchi, T. S.: Comparison of two methods for the analysis of lignin in marine sediments: CuO oxidation versus tetramethylammonium hydroxide (TMAH) thermochemolysis, Org. Geochem., 39(10), 1454–1461, 2008.

Yang, L., Guo, W., Chen, N., Hong, H., Huang, J., Xu, J. and Huang, S.: Influence of a summer storm event on the flux and composition of dissolved organic matter in a subtropical river, China, Appl. Geochem., 28(0), 164–171, 2013.

Table 1. Changes in discharge, DOC concentration and DOM compositional proxies during the storm events. The values are given for the first, peak discharge and final samples.

Event		**2**	**3**	**4**	**5**	**6**
Date		**Dec 4, 2010**	**Dec 19, 2010**	**Jan 6, 2011**	**Feb 13, 2011**	**Feb 19, 2011**
Discharge ($L\ s^{-1}$)	beg. [a]	79.8	88.8	59.1	72.8	77.7
	max.	177.3	453.1	169.8	167.3	245.1
	end	127.4	113.1	104.0	96.2	102.5
DOC ($mg\ L^{-1}$)	beg. [a]	7.4	6.6	6.4	7.4	8
	max.[b]	11.6	12.4	11.5	12.8	15.5
	end	9.8	7.4	8.0	11	9.1
SUVA ($L\ mg^{-1}\ cm^{-1}$)	beg. [a]	2.0	2.6	2.8	2.0	2.4
	max.[b]	3.1	3.3	3.4	3.2	2.9
	end	3.0	3.4	3.5	3.0	2.9
Plant-derived markers (%)	beg. [a]	31	49	31	14	31
	max.[b]	67	78	70	71	59
	end	57	72	58	60	25
deoxyC6/C5	beg. [a]	1.6	1.5	1.6	2.7	1.9
	max.[b]	0.9	1.1	1.0	1.1	1.3
	end	1.1	1.1	0.9	1.2	1.4
C/V	beg. [a]	0.2	0.2	0.2	0.2	0.3
	max.[b]	0.4	0.6	0.6	0.4	0.8
	end	0.5	0.5	0.4	0.4	0.3
Ac/Al (V)	beg. [a]	5.0	7.3	5.5	6.6	5.2
	max.[b]	5.2	5.3	4.6	5.5	4.5
	end	4.7	4.9	4.3	4.8	4.6

[a] Value recorded at the beginning of storm events.

[b] Value recorded at the peak discharge.

Figure captions

Figure 1. Location map of the Kervidy-Naizin critical zone observatory (Brittany, France). Grey areas located along the channel network indicate the maximum extent of the wetland zones. The global positioning system coordinates of the outlet are 48.0057 North, 2.8313 East (decimal degree).

Figure 2. Discharge (white area), daily rainfall (black area) and water table level in the wetland domain (dashed line) during the hydrologic year 2010-2011. Monitored storm events are indicated by numbers and arrows.

Figure 3. Temporal change of the molecular composition of inter-storm stream DOM: compositional ratios included C/V (white triangles - LIG-TAN), deoxyC6/C5 (black square – CAR) and the proportion of plant-derived markers among the analyzed compounds (black triangles).

Figure 4. Temporal change in flow and DOC concentration and composition during storm events 3 and 4. The units are given on the axes. The uncertainties for deoxyC6/C5, C/V and Ac/Al (V) are the mean RSD calculated for five samples analyzed in triplicate.

Figure 5. Temporal change in flow (dashed line) and proportion of plant-derived markers (black triangles) expressed as the percentage of analyzed compounds during storm event 5. The uncertainties are the mean RSD calculated for five samples analyzed in triplicate.

Figure 6. Time diagram comparing the variation of the C/V ratio (lignin proxy) in SOM and DOM from organo-mineral and mineral horizons, and the variation of the C/V ratio in river DOM during inter-storm and storm conditions.

Figure 7. Difference of the correlation between turbidity and the C/V ratio (lignin proxy) during the rising limbs (grey diamonds – p-value < 0.0001) and during entire storm events (grey and black diamonds – p-value = 0.008).

Figure 1

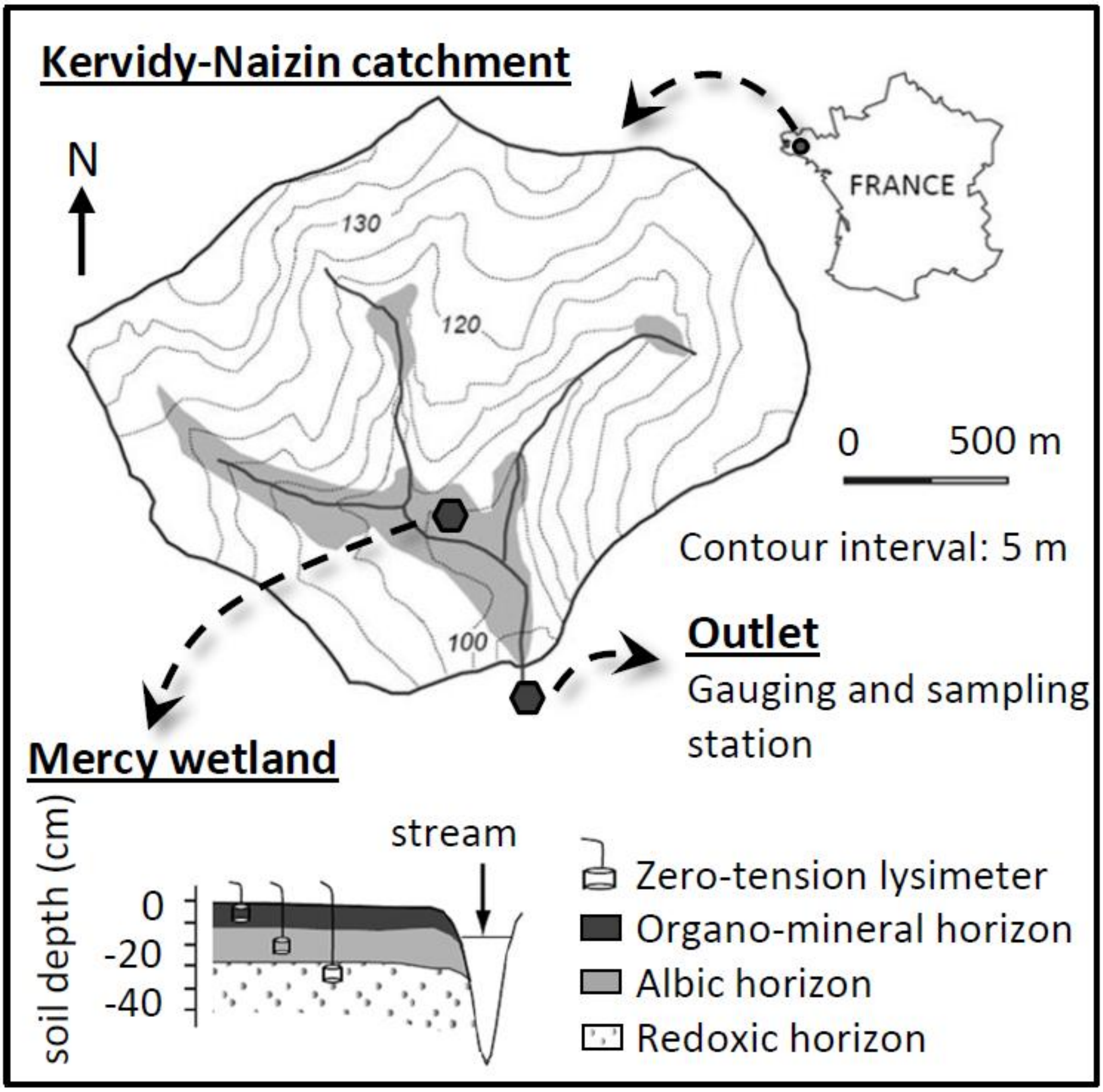
Kervidy-Naizin catchment
N
130
120
100
FRANCE
0
500 m
Contour interval: 5 m
Outlet
Gauging and sampling station
Mercy wetland
soil depth (cm)
0
-20
-40
stream
Zero-tension lysimeter
Organo-mineral horizon
Albic horizon
Redoxic horizon

Figure 2

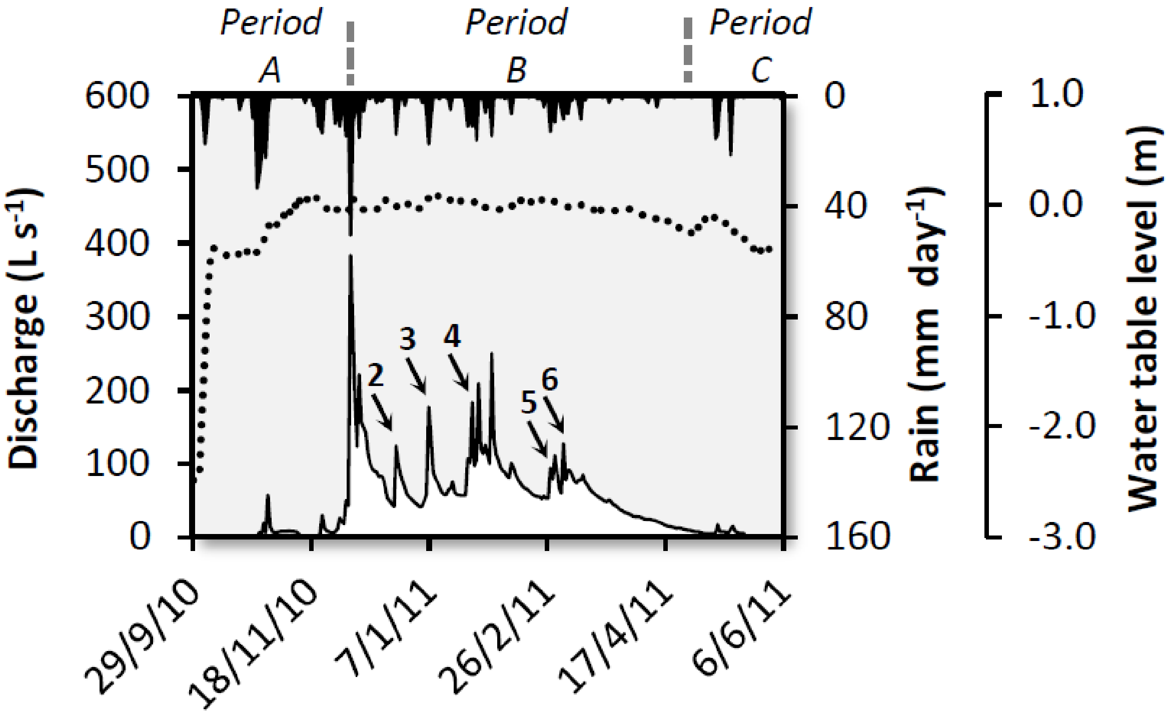
Period A
Period B
Period C
Discharge (L s-1)
600
500
400
300
200
100
0
Rain (mm day-1)
0
40
80
120
160
Water table level (m)
1.0
0.0
-1.0
-2.0
-3.0
2
3
4
5
6
29/9/10
18/11/10
7/1/11
26/2/11
17/4/11
6/6/11

Figure 3

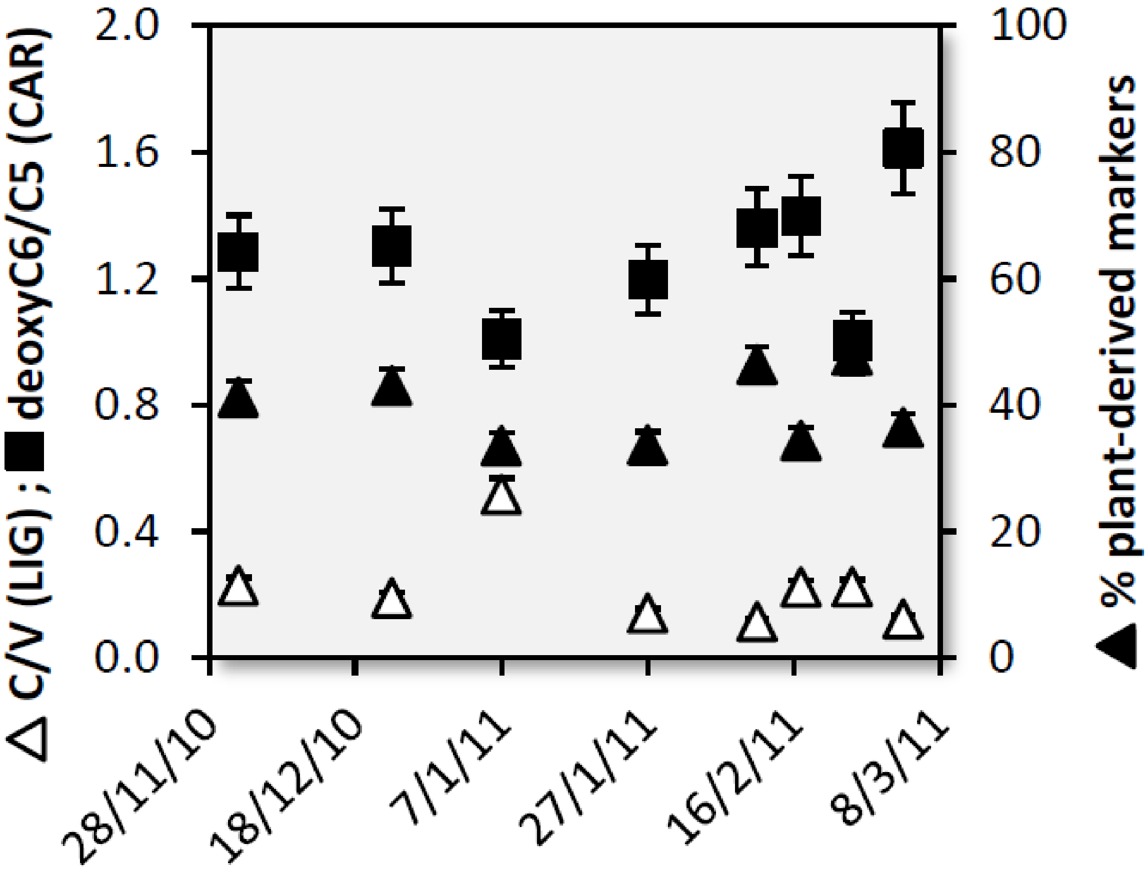
△ C/V (LIG) ; ■ deoxyC6/C5 (CAR)
2.0
1.6
1.2
0.8
0.4
0.0
100
80
60
40
20
0
▲ % plant-derived markers
28/11/10
18/12/10
7/1/11
27/1/11
16/2/11
8/3/11

Figure 4

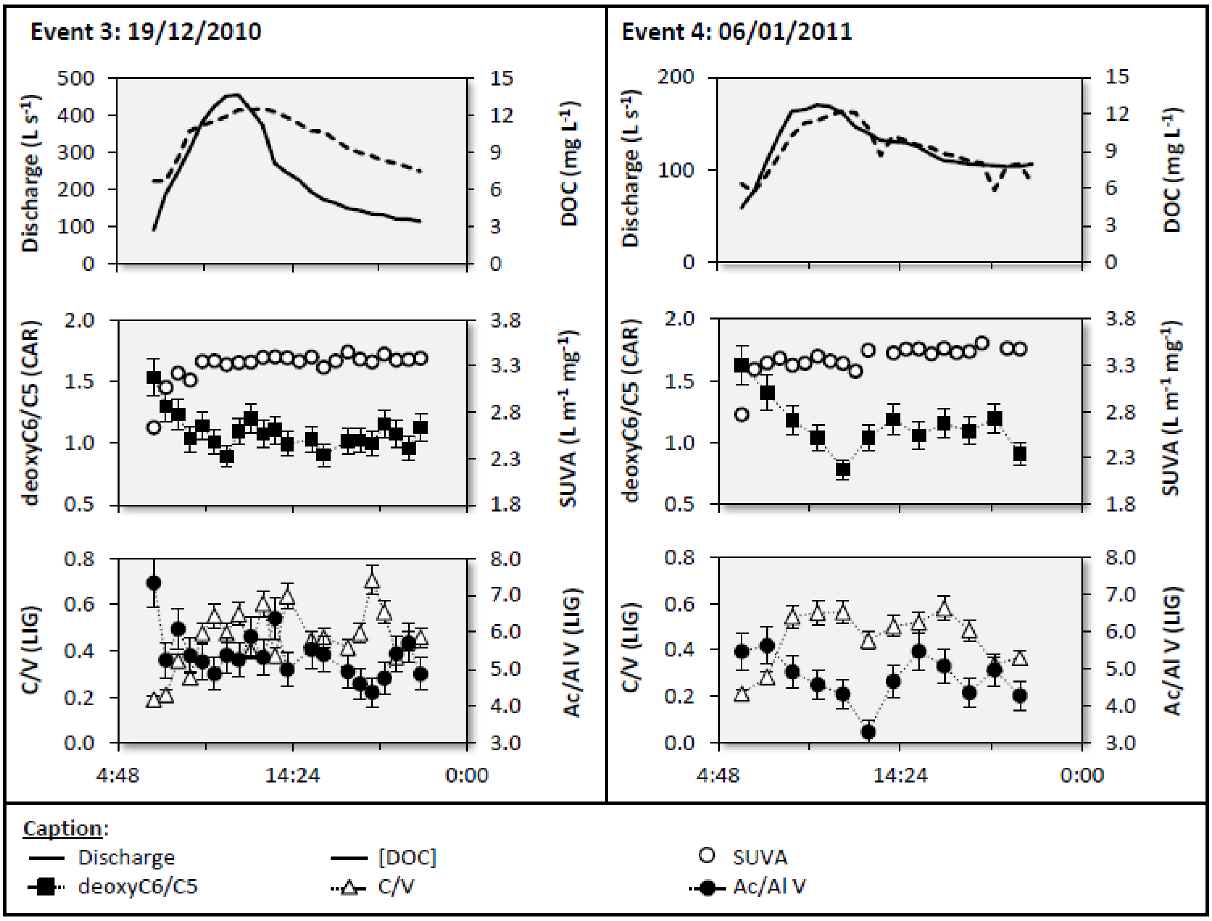
Event 3: 19/12/2010
Event 4: 06/01/2011
Discharge (L s-1)
DOC (mg L-1)
500
400
300
200
100
0
15
12
9
6
3
0
200
100
0
deoxyC6/C5 (CAR)
SUVA (L m-1 mg-1)
2.0
1.5
1.0
0.5
3.8
3.3
2.8
2.3
1.8
C/V (LIG)
Ac/Al V (LIG)
0.8
0.6
0.4
0.2
0.0
8.0
7.0
6.0
5.0
4.0
3.0
4:48
14:24
0:00
Caption:
Discharge
[DOC]
SUVA
deoxyC6/C5
C/V
Ac/Al V

Figure 5

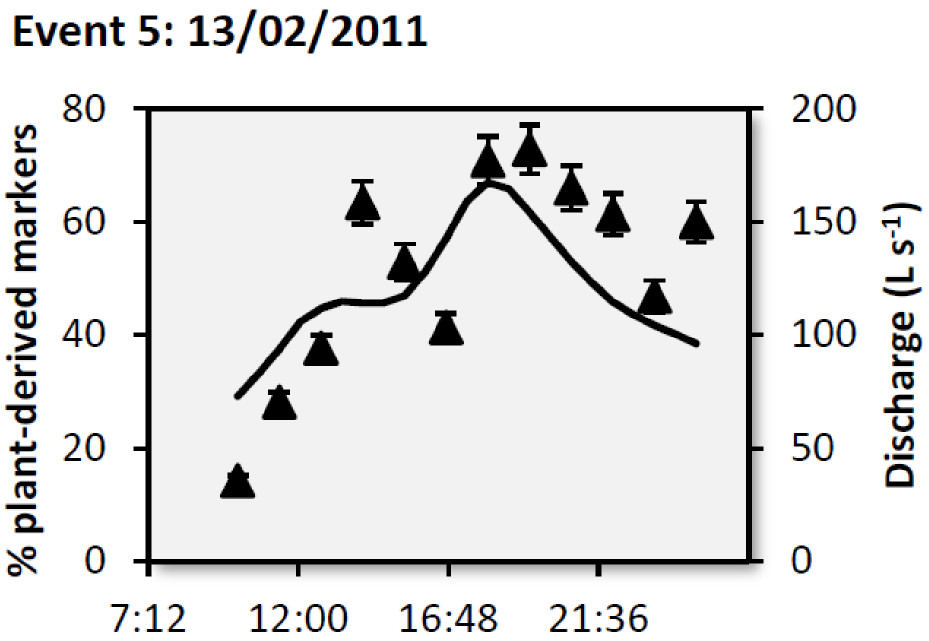
Event 5: 13/02/2011
% plant-derived markers
80
60
40
20
0
Discharge (L s^{-1})
200
150
100
50
0
7:12
12:00
16:48
21:36

Figure 6

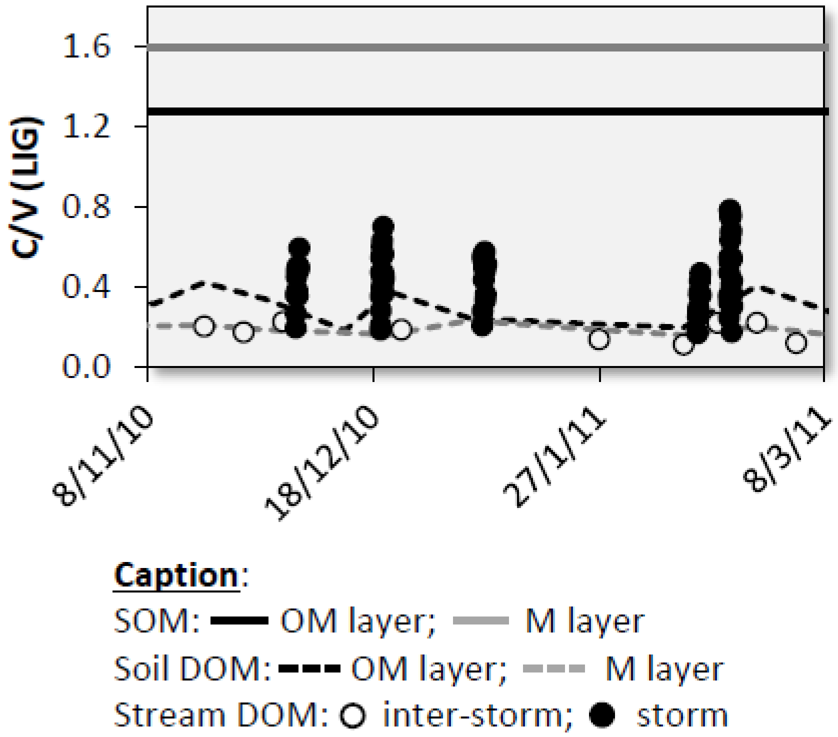
C/V (LIG)
1.6
1.2
0.8
0.4
0.0
8/11/10
18/12/10
27/1/11
8/3/11
Caption:
SOM: OM layer; M layer
Soil DOM: OM layer; M layer
Stream DOM: ○ inter-storm; ● storm

Figure 7

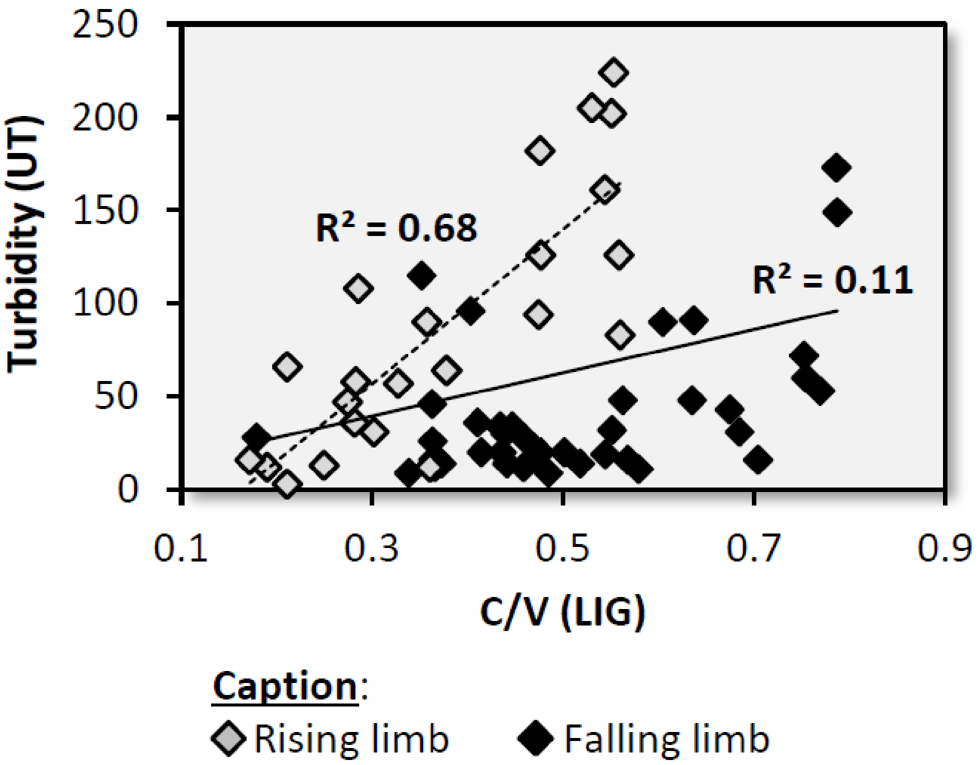
Turbidity (UT)
250
200
150
100
50
0
0.1
0.3
0.5
0.7
0.9
C/V (LIG)
R² = 0.68
R² = 0.11
Caption:
◇ Rising limb
◆ Falling limb